



Three-dimensional distribution of fine particulate matter concentrations and synchronous meteorological data measured by an unmanned aerial vehicle (UAV) in Yangtze River Delta, China

Si-Jia Lu¹, Dongsheng Wang¹, Xiao-Bing Li¹, Zhanyong Wang¹, Ya Gao¹, Zhong-Ren Peng^{1,2}

- 5 ¹ Center for UAV Application and ITS Research, State Key Laboratory of Ocean Engineering, School of Naval Architecture, Ocean & Civil Engineering, Shanghai Jiao Tong University, Shanghai, 200240, China
² Department of Urban and Regional Planning, University of Florida, Gainesville, FL 32611-5706, USA

Correspondence to: Z. R. Peng (zpeng@dcp.ufl.edu)

Abstract. Three-dimensional distribution of fine particulate matter (PM_{2.5}) and meteorological factors are of great
10 importance to clarify the formation mechanism of haze pollution and to help forecast atmospheric pollution under different
meteorological conditions. The objective of this study was to measure PM_{2.5} concentrations and meteorological data at 300-
1000 m altitude using an unmanned aerial vehicle (UAV) equipped with mobile instruments. The study was conducted in
a 4 × 4 km² space in Lin'an, Yangtze River Delta (YRD), China. The UAV was operated repeatedly for four times in one
day along the designed route spirally from the ground to 1000 m altitude with a total of 8 layers and a 100m interval between
15 two adjacent layers for five days from 21th August 2014 to 2nd February 2015. PM_{2.5}, air temperature, relative humidity,
dew point temperature and air pressure were measured during the data collection. The study results indicated that the PM_{2.5}
concentrations decreased with altitude at 300-1000 m and the variations of PM_{2.5} with altitude in morning flights were much
bigger than in afternoon flights. Besides, the PM_{2.5} concentration levels in morning flights were generally lower than in
afternoon flights. PM_{2.5} concentrations were positively correlated with dew point temperature and pressure, but positively
20 correlated with relative humidity only on pollution days in autumn or winter. The vertical gradient of PM_{2.5} concentrations
was small in pollution days compared with on clean days. These findings provide the key theoretical foundation for PM_{2.5}
pollution forecast and environmental management.

1 INTRODUCTION

Ambient air pollution is a primary environmental problem in industrial and developing countries, and China is not spared
25 (Ouyang et al., 2013). Among all the air pollutants, the fine particulate matter is responsible for the climate change and
visibility degradation (Davidson et al., 2005). What's more, the fine particulate matter pollution threatens the human health,
especially cardiorespiratory system (Pope et al., 2002, 2009; Dominici et al., 2006).

Studying the formation and dissipation mechanism of fine particulate matter is of significance for air pollution forecast and
urban planning. However, most of the previous studies mainly focused on the characteristics of fine particulate matter on



surface level. The only ground-based observations were not sufficient for further research of the trans-boundary transport of pollutants (Ding et al., 2009), the influence of atmospheric microcirculation (e.g. sea-land breeze, urban heat island effect) on pollutant distribution in urban area (Strawbridge et al., 2004), and calibration of atmospheric model (Boy et al., 2006; Ding et al., 2009).

- 5 Studies of the particulate matter (PM) vertical concentrations in troposphere and planetary boundary layer (PBL) were routinely conducted by meteorological tower (Ding et al., 2005; Yang et al., 2005; Gao et al., 2012; Sun et al., 2013), tethered balloon (Clark et al., 2000; Maletto et al., 2003; McKendry et al., 2004), LiDAR (Strawbridge et al., 2004) and manned aircraft (Wang et al., 2008). Meteorological tower monitoring is fit for long-term continual observations, but it is limited to monitoring elevation (no more than 350 m) and mobility. Ding et al. (2005) and Yang et al. (2005) found that
- 10 $PM_{2.5}$ mass concentrations logarithmically decreased with increasing altitude. Ding et al. (2005) also classified the $PM_{2.5}$ vertical distribution in Beijing into two patterns: gradual decline pattern and rapid decline pattern. However, Sun et al. (2013) indicated that the reverse distribution of relative humidity (RH) might result into a “higher-top and lower-bottom” pattern of $PM_{2.5}$ distribution, considering moisture absorption effect of particulate matter. Tethered balloon monitoring could overcome some drawbacks of meteorological tower monitoring and could obtain PM concentrations at continuous height levels.
- 15 Nevertheless, it is restricted to the horizontal monitoring range. Maletto et al. (2003) indicated that fine particulate matter ($PM_{2.5}$) tended to be well mixed vertically during daytime whereas coarse particulate material (PM_{10}) tended to be found close to ground and sources due to gravitational settling. While Mckendry et al. (2004) claimed that layers of fine particulate matter may be found in wintertime nocturnal settings. LiDAR is a simple and efficiency method to monitoring the PM concentrations in the whole atmosphere indirectly. Strawbridge et al. (2004) discovered that increased PM concentrations in
- 20 the Northeastern valleys during the night flights due to a persistent sea breeze. Compared with the methods discussed above, manned aircraft monitoring is responsible for a large area of monitoring. Wang et al. (2008) found that fine particles are dominant fraction of particulate matter in the troposphere and $PM_{2.5}$ concentration distribution is close association with boundary-layer structure and changing of wind.

- To better understand and study the dispersion and distribution of PMs, there are several commonly used methods, among
- 25 which unmanned aircraft vehicle monitoring (UAVM) is a state-of-the-art technique. In terms of cost-efficiency, UAVM has an advantage compared with manned aircraft monitoring. Unmanned aircraft monitoring platform (UAMP) were recently applied for monitoring meteorological data (Kroonenberg et al., 2008, Wildmann et al., 2013; Wildmann et al., 2014; Altst ätter et al., 2015), atmosphere structure (Thomas et al., 2012; Wildmann et al. 2014; Lothon et al. 2014) and particulate matter (Clarke et al., 2002; Harnisch et al., 2009; Bates et al., 2013; Altst ätter et al., 2015). Clarke et al. (2002) indicated
- 30 that UAMP is of good quantitative performance under a range of conditions and is able to provide reliable partially dried size distributions. Ramana et al. (2007) found that the simulated clear sky heating rates are consistent with the broadband heating rates observed by stacked aircraft within experimental errors (about 15%). Harnisch et al. (2009) discovered an asymmetry in the aerosol distribution in the cross-valley direction and he presumed that it is related to differences in orientation and albedo of the two valley slopes. Bates et al. (2013) found that frequent aerosol layers aloft with high PNC and enhanced



aerosol light absorption. Altstalter et al. (2015) discovered that a particle burst event occurred during the boundary layer development in the morning. In summary, most research focused on the vertical distributions of PM concentrations, but few studied the three-dimensional distribution of PM, especially during the formation and dissipation events.

In our research, a fixed-wing unmanned aircraft vehicle (UAV) was modified from an air-mapping aircraft with the payload capacity of ~5kg. The sensors for PM concentrations and meteorology were calibrated and tested in the laboratory. The UAV research was operated to investigate three-dimensional distribution of PM concentrations both spatially and temporally. 20 monitoring flights in five days across over a half year were totally done over suburban area of Lin'an in YRD. The observations were conducted in the lower troposphere, especially within the atmospheric boundary layer. The daily variety of PM_{2.5} in the atmosphere were captured and the accumulation and dissipation of PM_{2.5} is discussed in this article. This study provides detailed measurements of the small-scale three-dimensional variability of the PM_{2.5} concentrations.

2 EXPERIMENTS AND METHODS

2.1 Experimental Site

Mobile vertical monitoring were performed in a $4 \times 4 \text{ km}^2$ suburban area in the north part of Lin'an, China (E 118°51'-119°52', N 29°56'-30°23') (see Figure 1). The experimental site is approximately 13 km from Lin'an downtown. A highway runs west-to-east across the experimental area. Some machinery manufacture plants are located on the south side of the highway. No direct pollution sources are within or near around the experimental area. There is a relative low density of houses in this area and only hills are surrounded on the southeast and northwest of the area. In the experimental area, nearly half of the ground is covered by trees and one-third of the surface is bare land.

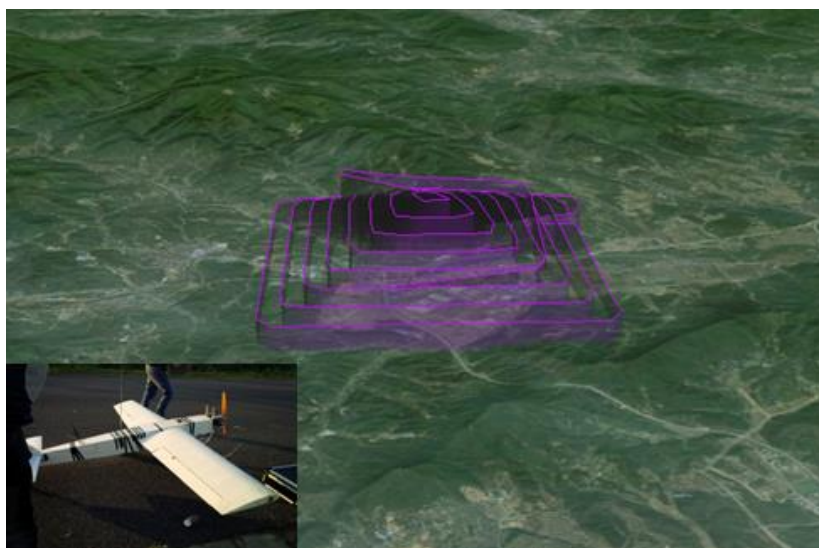


20 **Figure 1.** Experimental site in Lin'an, China.



2.2 Mobile Monitoring

Mobile vertical monitoring was performed with an Unmanned Aerial Vehicle (UAV) equipped with fast-response instruments for monitoring fine particulate matter concentration ($PM_{2.5}$) and meteorology (see Figure 2). The UAV has a 2-meter wingspan range and is powered by an engine that is exhausted above the nose of the UAV. The UAV was controlled by its pilot when it took off and lands on the road. As it flies to 300 meters high, manipulator switched over to autopilot. The UAV climbed spirally from 300 m to more than 1 km altitude along the designed route at a constant speed ~120 km/h. Typically, one flight lasts for about 45 minutes so that it can collect enough data at each vertical altitude level.



10 **Figure 2. UAV and its flight route.**

$PM_{2.5}$ concentrations were measured using TSI Sidepak AM510 PM Detector. Air temperature (T), relative humidity (RH) and dew point temperature were measured with HOBO U12 Temp/RH Data Logger, which is fixed outside the fuselage. Black carbon (BC) and pressure was measured with an aethalometer. Latitude, longitude and height was recorded by Columbus V-900 Multifunction GPS receiver. The measurement equipment is listed in Table 1. No measurements for dew point temperature were recorded during the flight-2 to -4 on 21th August 2014 due to equipment failures.

Table 1. Particles and Meteorology Monitoring Equipment on UAV.

Parameter	Equipment	Detection limit	Instrument reporting interval (s)
$PM_{2.5}$	TSI SIDEPACK AEROSOL	0.001mg/m ³	2



MONITOR AM510

Air temperature	HOBO Temperature and	0.03 °C	
Relative humidity	Relative Humidity Probe	0.03%	2
Dew point		0.03 °C	
Black carbon (BC) pressure	Aethlabs AE51	0.001 µg/m ³	1
Latitude	Columbus V-900		
longitude	Multifunction GPS Data		1
height	Logger		

The particle mass concentration instruments were taken to the Shanghai Environmental Monitoring Center for a direct comparison with the TEOM mass measurement devices on the ground. The results detected by our monitoring instruments are quite consistent with the TEOM data, and the correlation coefficient is more than 0.95.

- 5 Three-dimensional monitoring was performed on a total of 5 days on August 21th, October 11th, November 14th, December 12th in 2014 and February 5th in 2015 including 16 flights (see Table 2). Four flights were done on each monitoring day. Flight-1 was assigned after sunrise; flight-2 was assigned before noon; flight-3 was assigned at noon; flight-4 was assigned before dusk. Effective monitoring time during a flight was about 30-40 minutes.

10 **Table 2. Flight Monitoring Times and Dates.**

Date	Flight time	Weather conditions	PM _{2.5} ($\frac{\mu\text{g}}{\text{m}^3}$)	Temperature(°C)	Humidity(%)	WD/ WS
2014-8-21	6:26-7:00	Cloudy	25	20	99	SW/2
	10:17-10:52	Cloudy	23	25	78	SE/1
	14:11-14:46	Cloudy	15	30	60	NE/2
	16:22-16:57	Cloudy	16	30	58	E/2
2014-10-11	7:32-8:09	Cloudy	46	21	86	E/2
	10:02-10:39	Cloudy	28	23	63	NE/3
	14:00-14:35	Cloudy	23	26	52	E/3
	15:47-16:22	Cloudy	27	24	57	NE/3
2014-11-14	7:28-8:01	Cloudy	46	3	89	SW/1
	10:02-10:37	Cloudy	48	12	53	SE/1
	14:02-14:37	Cloudy	44	16	34	NE/3
	15:33-16:07	Cloudy	51	15	34	NE/3
2014-12-12	8:08-8:46	Sunny	104	2	87	SE/1
	10:35-11:17	Sunny	95	5	41	N/1



	14:22-15:02	Sunny	37	9	26	W/3
	15:32-16:13	Sunny	33	8	27	W/3
2015-2-5	8:08-8:45	Cloudy	151	0	89	NE/1
	10:44-11:21	Sunny	190	5	51	E/1
	14:14-14:50	Sunny	36	8	31	N/3
	15:25-15:59	Sunny	28	7	31	E/3

Before each take-off, the status of instruments were checked such as remaining battery and storage space, and each inlet tubing at curve was inspected whether it was compressed. The PM_{2.5} and RH monitors were allowed to warm up for at least 20 min prior to calibration. In cold temperature (<10°C), the warm-up time was extended to 35-40 min to ensure stable readings. After the instruments had warmed up, the calibrations were checked to zero (Padró-Martínez et al., 2012). The calibrator controls the flow of calibration gases and generates zero PM_{2.5}. The particle inlet manifold was made of stainless steel. All tubing on instrument inlets was either Tygon or conductive-silicon tubing. The length of tubing from the manifold to each instrument was minimized to reduce particle loss due to sorption.

Background data including hourly PM_{2.5} mass concentrations, humidity, temperature, wind speed and wind direction, was obtained from the Air Quality On-line Monitoring and Analysis Platform of China (<http://www.openair-project.org/Examples/WindPollutionRoses.aspx>). These data are offered by the Meteorological Bureau of Lin'an. The sounding data, including air temperature, dew point temperature, relative humidity, wind speed and wind direction, was downloaded from the website of department of atmospheric science, University of Wyoming (obtained at <http://weather.uwyo.edu/upperair/sounding.html>). These sounding meteorology data was observed by the sounding station located in Hangzhou, China, which is ~40 km away from the experimental site and the timing sounding is operated at 12:00 every day.

2.2 Data Processing and Analysis

PM_{2.5} concentration data collected with the instruments was exported by TrakPro v4.7.0. Then, the exported data was aggregated in MySQL using R scripts. Post-processing for quality control was performed using Excel VBA macros and by inspection of time-series plots. Data processing consists of several steps. First, measurements associated with instrument errors, as noted in the flight log, were removed. The next step was to remove data that reflected self-monitoring of exhaust from the UAV. Self-monitoring was possible when the UAV was taking off and descent. Self-monitoring can be minimized by locating the gas and particle inlets below the bottom of the vehicle near the rear of the UAV and adjusting flight attitude. Based on the height information provided by the airborne GPS sensor, data collected below 300 m altitude and during descent stage was excluded. Overall, 18% of the data from each monitoring flight was removed due to self-monitoring.



Considering that instruments that measuring $PM_{2.5}$ concentrations is based on light scattering principle, the observed concentrations can be impacted by relative humidity (Mamouri et al., 2013). Thus, a correction factor (CF) is used to compensate this error. The results fit the actual data quite well after the correction (Day et al., 2000). CF is expressed as follows:

$$CF = 1 + \frac{RH^2}{4(1-RH)} \quad (1)$$

where, RH denotes relative humidity.

All the raw data was averaged to 10 seconds in order to facilitate data calculation and interpretation. Then, the 10-second-averaged data was averaged for each height layer.

3 RESULTS AND DISCUSSION

10 3.1 Spatial and Temporal Distribution of Particle Mass Concentration

Figure 3 shows the spatial distributions of $PM_{2.5}$ mass concentrations measured during 20 flights. From the horizontal space analysis, the $PM_{2.5}$ concentrations at different altitudes of horizontal layers are different, but the difference in vertical distribution is more significant than in horizontal distribution. The $PM_{2.5}$ concentrations were different at different altitudes, and the spatial distributions are also different at different times of the day. The averaged vertical profiles of $PM_{2.5}$ concentrations are illustrated in Figure 4.

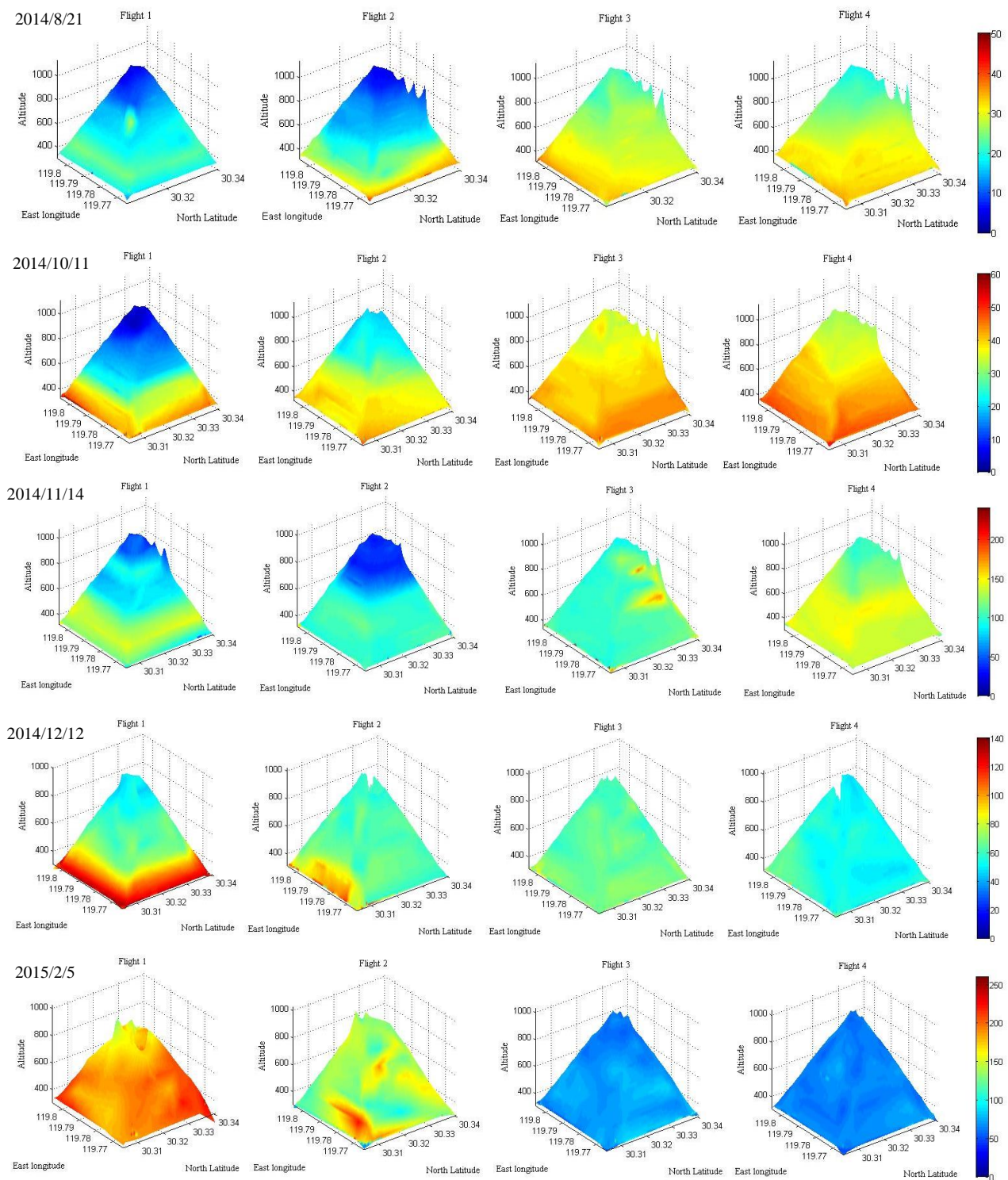


Figure 3. Spatial distribution of PM_{2.5} concentrations.



For the sake of simplicity, flight-1 and flight-2 were grouped as morning flights and flight-3 and flight-4, afternoon flights. In general, $PM_{2.5}$ concentrations measured in both morning flights and afternoon flights decrease with altitude increasing, which depicts a “higher-bottom and lower-top” pattern (Šmídl et al., 2013). This is consistent with the findings of tower observations (Liao et al., 2014). However, the vertical distribution pattern in morning flights is different from that in afternoon flights (see Figure 4). These observations indicate that the atmosphere boundary layer (ABL) height has a significant impact on the $PM_{2.5}$ concentration vertical distribution. The PBL height is relatively low at night and in the early morning. This leads to a fact that the $PM_{2.5}$ near the ground cannot be transported to the high altitude. There is a relative big difference between 300 m and 1000 m in flight-1, compared with flight-2, -3, and -4 (see Figure 4). With the PBL height increasing rapidly in the morning and reaching its peak value in the afternoon, atmosphere convection is strengthened. Thus, $PM_{2.5}$ near the ground and in the high altitude is mixed and its concentration vertical distribution in afternoon flights tends to be homogeneous. Linear regression is conducted to illustrate the vertical gradient of $PM_{2.5}$ concentrations (see Table 3). The absolute values of the vertical gradients in morning flights are apparently more than that in the afternoon flight (about 1.68–13 times). The $PM_{2.5}$ concentration average at 300–1000 m altitude in the afternoon is higher than in the morning, likely reflecting atmospheric turbulence contribution to particulate matter concentration in the afternoon, which is consistent with findings of Ding (Ding et al., 2005). In flight-1 on pollution days (2014/11/14, 2014/12/12, and 2015/2/5), the vertical gradients of $PM_{2.5}$ concentrations range from -0.1281 to -0.10. While in flight-2, the vertical gradients of $PM_{2.5}$ concentrations range from -0.0397 to -0.0379, both on pollution and clean days, except for -0.1381 on 14th November, and -0.022 on 12th December. The vertical gradients of $PM_{2.5}$ concentrations ranged from -0.0178 to -0.0076. However, the gradients fluctuate violently in flight-4.

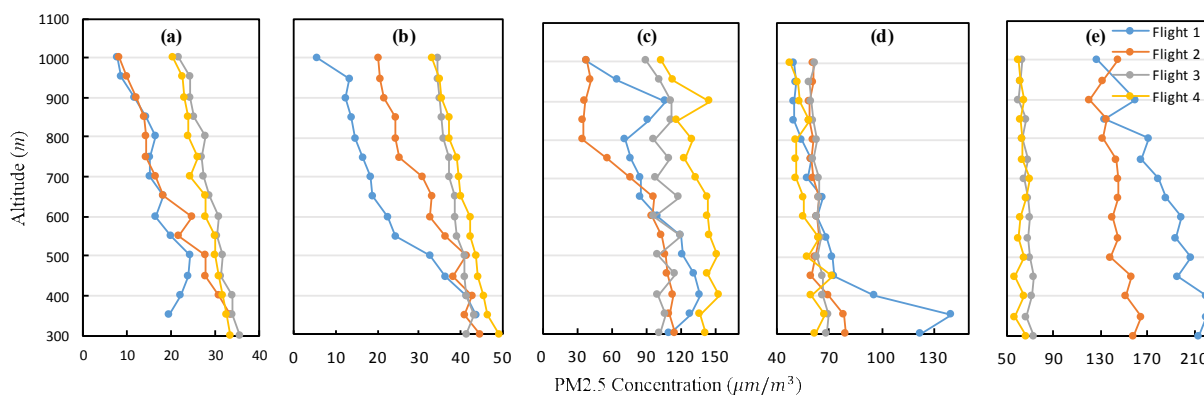


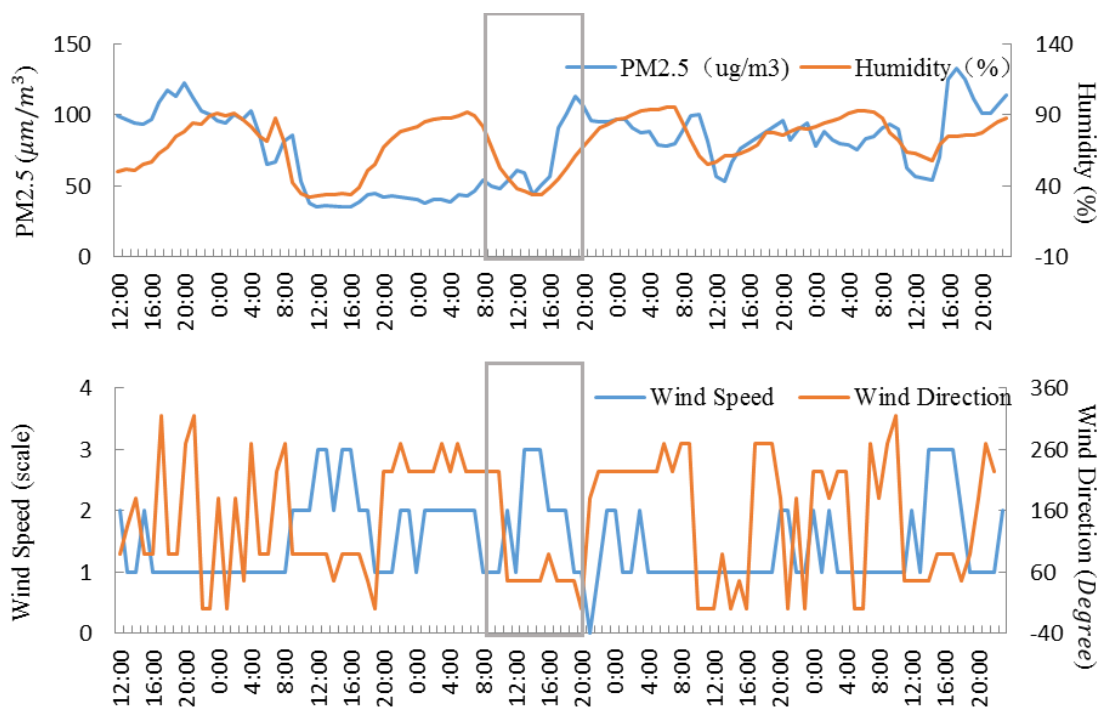
Figure 4. $PM_{2.5}$ mass concentration profiles of all the flights. Flights 1-4 during a monitoring day are marked with blue, red, gray and yellow, respectively. (a) 2014/8/20; (b) 2014/10/11; (c) 2014/11/14; (d) 2014/12/12; (e) 2015/2/5.



Table 3. Vertical Gradient of PM_{2.5} Concentrations ($\mu\text{m}/\text{m}^4$).

	Flight-1	Flight-2	Flight-3	Flight-4
2014/8/21	-0.022	-0.0382	-0.0178	-0.018
2014/10/11	-0.0541	-0.0379	-0.01276	-0.0206
2014/11/14	-0.1027	-0.1381	-0.0076	-0.0478
2014/12/12	-0.102	-0.0225	-0.0127	-0.232
2015/2/5	-0.1281	-0.0397	-0.014	0.0011

3.2 Accumulation Event for PM_{2.5} (2014/11/14)



5 **Figure 5. PM_{2.5} concentration, relative humidity, wind speed and wind direction on 12th-16th November.**

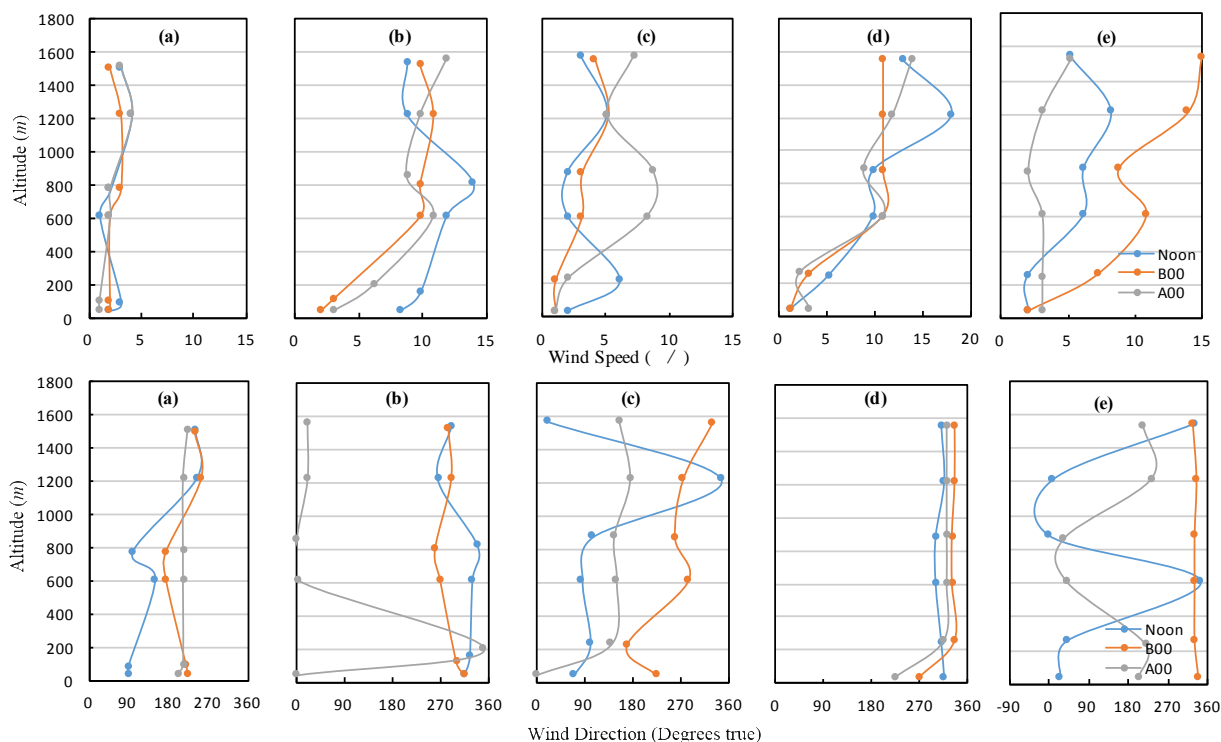


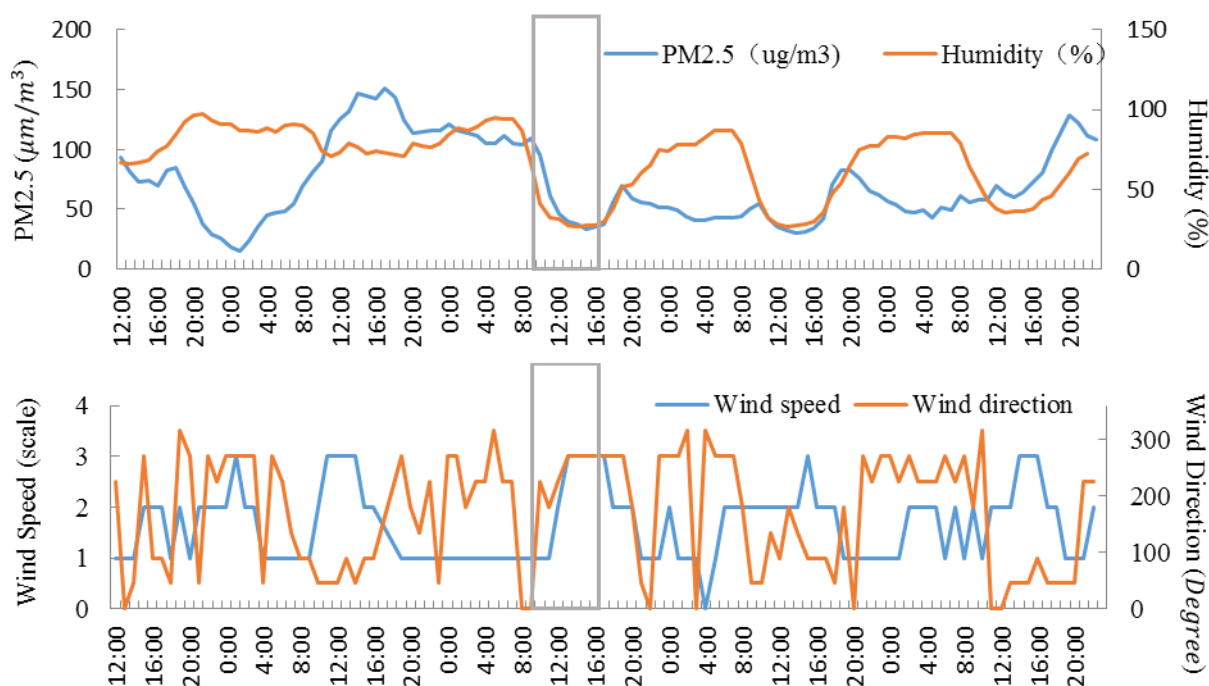
Figure 6. Wind speed and wind direction in 0-1800 m altitude by sounding.

Figure 5 shows time series of hourly averaged $PM_{2.5}$ concentrations and relative humidity at the ground level from 12th to 16th November 2014. Fine particulate matter accumulated from 14:00 on 14th November and its concentration climbed to peak value $\sim 113 \mu g/m^3$ at 19:00 on 14th November. 14th November was the static stability weather (see Figure 9 (c)). Wind speed at 0-1800 m altitude was mainly less than 5 m/s which was unfavorable for dispersing air pollutants horizontally and wind was from east below 900 m and from north upper 900 m. Our monitoring campaign was operated during the pollution accumulation stage, starting from 7:30 to 16:00, including four flights. During flight-1 (7:28-8:01), $PM_{2.5}$ concentrations exhibit a positive vertical gradient at 300-400 m and 800-900 m altitude. This can be explained by thermal inversion layer. Seen from Figure 9 (c), dew point temperature displays a positive vertical gradient at 300-400 m and 700-900 m. This reflects that shallow thermal inversion layer formed at these two altitude layers, leading to the steady atmospheric stratification and plenty of moisture. Fine particulate matter can be transported to the top of thermal inversion layer and mixed well, but can be obstructed to continue upward by thermal inversion layer. During flight-2 (10:02-10:37), $PM_{2.5}$ concentrations show a stable negative gradient ~ -0.054 below 650 m, but sharply increase to ~ -0.399 at 650-800 m. This is due to weak clean air from the north that diluted the air pollution. The mean $PM_{2.5}$ concentrations at 300-1000 m altitude generally increase from $98.13 \mu g/m^3$ in flight-1 to $134 \mu g/m^3$ in flight-4 (15:33-16:37). This is because air humidity



increases apparently with the wind direction changing from north to west, which accelerates the coagulation of particle matter.

3.3 Dissipating Event for PM_{2.5} (2014/12/12 and 2015/02/05)



5 **Figure 7. PM_{2.5} concentration, relative humidity, wind speed and wind direction on 10-14 December.**

Figure 7 shows that monitoring campaign on 12th December captured the dissipating process of PM_{2.5}. Particle matter accumulated at 00:00 on 11th December and this pollution lasted about 9 hours and began to dissipate at 9:00 on 12th December. At about 15:00 on 12th December, PM_{2.5} reached its minimum 33 $\mu\text{g}/\text{m}^3$. PM_{2.5} concentrations exhibit a positive vertical gradient at 300-350 m altitude in flight-1. The phenomenon can be explained by the shallow thermal inversion layer at 300-350 m (see Figure 9 (d)). In flight-1, PM_{2.5} concentration gradient was ~ -0.662 at 350-400 m altitude, while increased to -0.123 at 450-1000 m altitude. During all the four flights, wind direction was of great consistency but the wind speed increased with altitude.

10

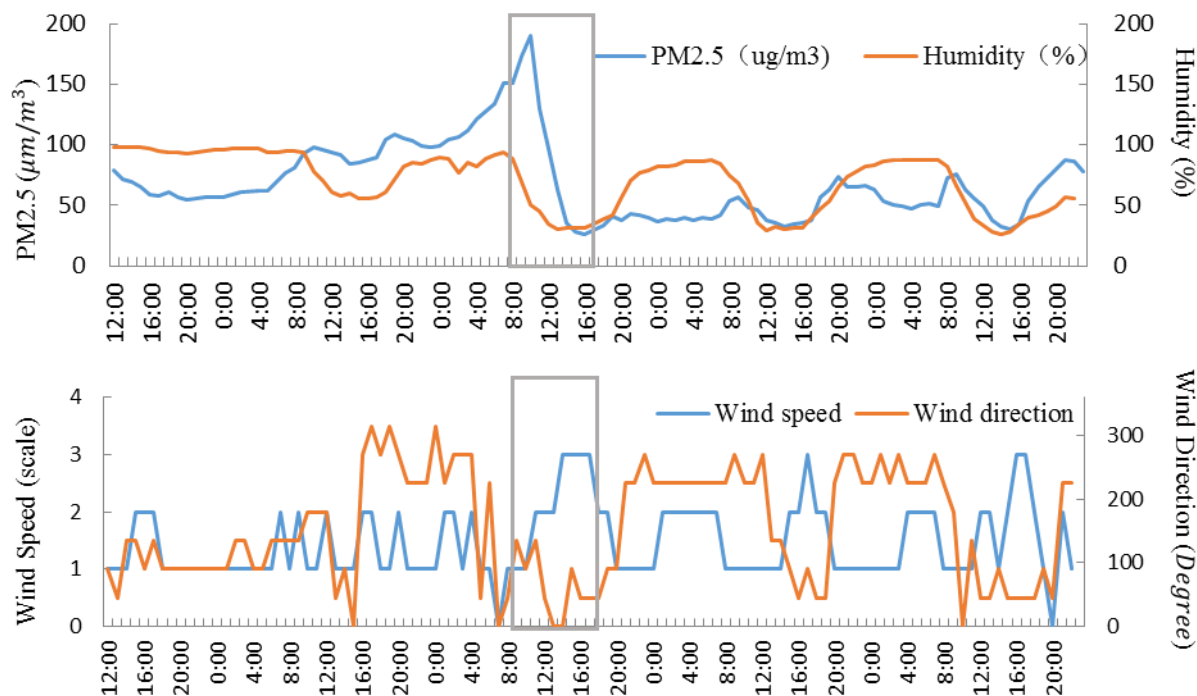


Figure 8. PM_{2.5} concentrations, humidity, wind speed and wind direction on 3th-7th February.

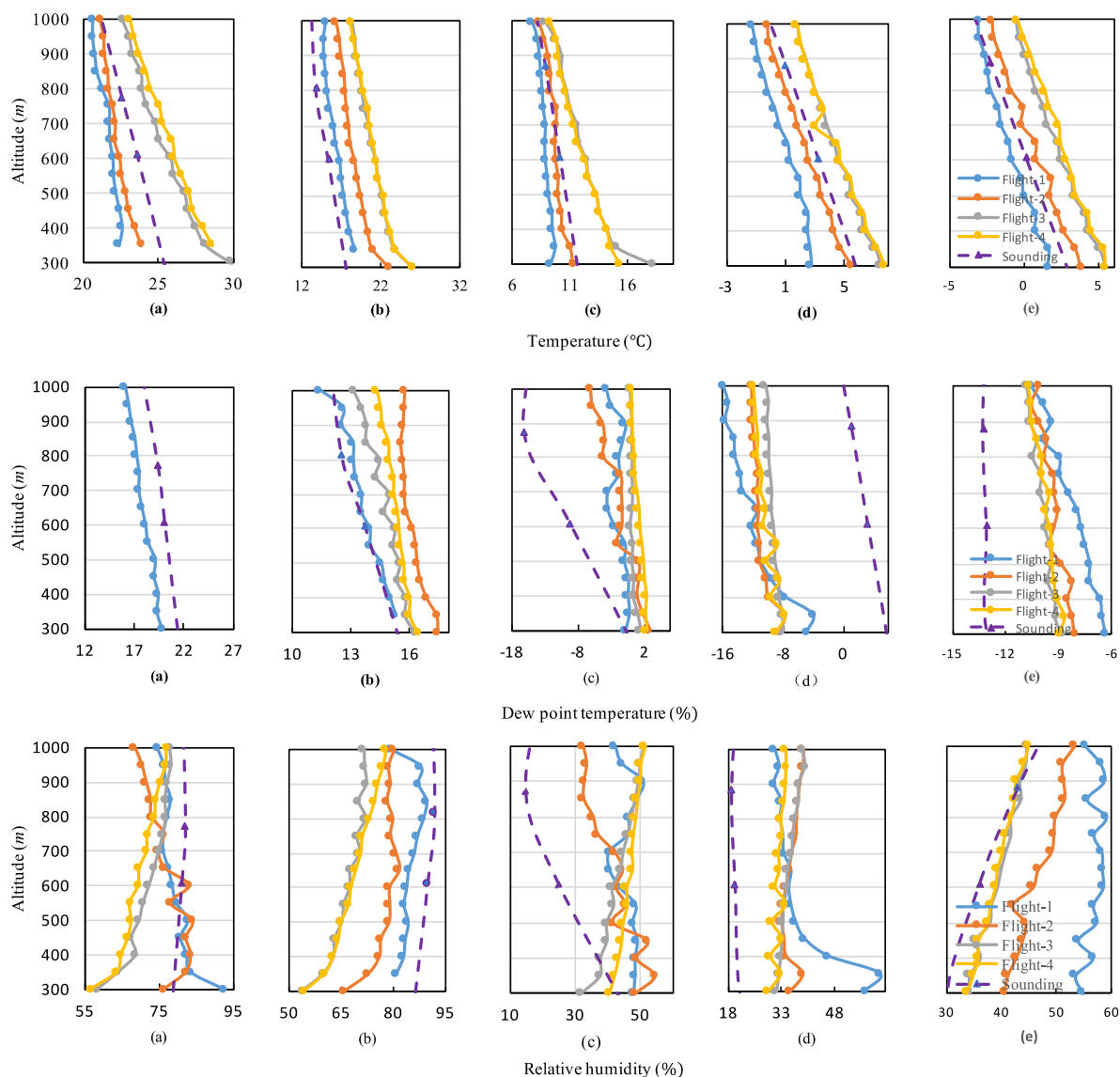
Monitoring campaign on 2nd February also captured the dissipation process of PM_{2.5} (see Figure 8). Particle matter was accumulating at 06:00 on 4th February and remained 70-100 $\mu\text{g}/\text{m}^3$. Then, PM_{2.5} concentrations started to enhance at 00:00 on 5th February and climbed to peak value $\sim 190\mu\text{g}/\text{m}^3$. In later 5 hours, PM_{2.5} concentration decreased sharply from 190 $\mu\text{g}/\text{m}^3$ to 26 $\mu\text{g}/\text{m}^3$. PM_{2.5} concentrations generally show negative gradient in all four flights, -0.123, -0.019, -0.013 and -0.010 for flight-1 (8:08-8:45), -2 (10:44-11:21), -3 (14:14-14:52) and -4 (15:25-15:59), respectively. Wind speed at each height level increasing more than 50% and wind direction almost coming from north by east jointly led to the rapid reduction of PM_{2.5} at each height layer.

3.4 Meteorological Factors

The averaged vertical profiles of dew point temperature, temperature and relative humidity at 300-1000 m are illustrated in Figure 9. The sounding data collected at noon of the monitoring day is marked with dash lines in Figure 9. The sounding is performed at 12:00 that is between flight time of flight-2 and flight-3. The overall trend and data range of the sounding data are consistent with the data that measured by UAV during flight-1, except for that on 5th February which is more consistent with flight-2. This indicates that the UAV measurements are of feasibility and utility. What's more, UAV measurements



offer higher resolution observations than sounding. This provides us precise data for revealing the mechanism of air pollutions formation and dissipation and the relationships among particle matter and meteorological factors.



5 **Figure 9. Profiles of air temperature, dew point temperature and relative humidity measured by UAV (marked by solid lines) and by sounding (marked by dash lines).**(a) 2014/8/20; (b) 2014/10/11; (c) 2014/11/14; (d) 2014/12/12; (e) 2015/2/5.



To study the relationships among PM_{2.5} concentrations and meteorological parameters measured by the UAV, Pearson's correlations were calculated among them on the basis of mean values of each layer from 300 m to 1000 m. The obtained correlation coefficients are given in Table 4, together with their significance levels.

5 **Table 4. Pearson's Correlation Coefficients among PM_{2.5} Concentrations and Meteorological Parameters.**

		PM _{2.5}	Temp	RH	Dewpoint	Pressure
2014/8/21	PM _{2.5}	1	0.313**	-0.142**	0.032	0.750**
	Temp		1	-0.800**	-0.852**	0.140**
	RH			1	0.632**	-0.018
	Dewpoint				1	.223
	Pressure					1
2014/10/11	PM _{2.5}	1	0.761**	-0.666**	0.857**	0.583**
	Temp		1	-0.916**	0.742**	0.477**
	RH			1	-0.531**	-0.259**
	Dewpoint				1	0.797**
	Pressure					1
2014/11/14	PM _{2.5}	1	0.447**	0.319**	0.690**	0.497**
	Temp		1	-0.338**	0.664**	0.467**
	RH			1	0.477**	0.037
	Dewpoint				1	0.614**
	Pressure					1
2014/12/12	PM _{2.5}	1	-0.011	0.854**	0.764**	0.502**
	Temp		1	-0.364**	0.528**	0.686**
	RH			1	0.591**	0.147**
	Dewpoint				1	0.710
	Pressure					1
2014/2/5	PM _{2.5}	1	0.010	-0.001	0.068*	0.034
	Temp		1	-0.840**	0.005	0.833**
	RH			1	0.532**	-0.423**
	Dewpoint				1	0.513**
	Pressure					1

** Correlation is significant at the 0.01 level (one-tailed); * correlation is significant at 0.05 level (one-tailed).



The $PM_{2.5}$ concentrations positively correlate with dew point, air temperature and pressure. This indicates that the vertical distribution of dew point temperature has a remarkable positive impact on the vertical distribution pattern of $PM_{2.5}$. Notably, $PM_{2.5}$ concentrations negatively correlate with relative humidity in clean days (21th August and 11th October), but positively correlate in pollution days. The results verify that, in pollution days, the exceptional high relative humidity is a major inducing factor for the high fine particulate matter concentrations, especially in autumn and winter. This is consistent with previous studies (Ding et al., 2005; Bates et al., 2013).

4 CONCLUSIONS

This study is focused on characterizing microscope spatio-temporal patterns of $PM_{2.5}$ concentrations from 300 m to 1000 m altitude in a suburban area. The major findings are listed as follows: (i) In general, $PM_{2.5}$ concentration levels in the afternoon flights are higher than those in the morning flights, except February 5, 2015, on which day the relative humidity dropped rapidly in the late morning. (ii) Vertical distributions of $PM_{2.5}$ are non-uniform and the variations of $PM_{2.5}$ level regarding height in morning flights are much bigger than those in afternoon flights. (iii) Regional air pollution event, e.g., factory pollution and transportation-related pollution, has a great impact on the vertical distribution of the $PM_{2.5}$ concentrations. The vertical gradient of the $PM_{2.5}$ concentrations is smaller on pollution days than on clean days. (iv) The meteorological conditions are significantly related to the vertical distribution of the $PM_{2.5}$ concentrations. $PM_{2.5}$ concentrations are positively correlated with dew point temperature and pressure, which means that the vertical distribution of dew point temperature has a significantly positive impact on the vertical distribution pattern of $PM_{2.5}$. The high relative humidity level is the major inducing factor for the heavy air pollution, especially in autumn and winter.

However, it is challenging to measure meteorological factors and $PM_{2.5}$ data for consecutive 24 hours, considering the limitation of the endurance of the UAV and mobile instruments. Besides, the number of instruments carried by the medium-sized UAV is restricted. With these certain limitations in mind, our future studies will focus on resolving them and push this methodology onto a new level.

ACKNOWLEDGMENTS

The authors are grateful to Shanghai Environmental Protection Bureau, Shanghai Environmental Monitoring Center, Science Technology Department of Zhejiang Province (2014C31028), and the State Key Laboratory of Ocean Engineering of China at Shanghai Jiao Tong University for help with their support. The authors also express appreciation for the Second Surveying and Mapping Institute of Zhejiang Province for cooperation in manipulating the UAV for these experiments.



REFERENCES

- Altstalter, B., Platis, A., and Wehner, B.: ALADINA—an unmanned research aircraft for observing vertical and horizontal distributions of ultrafine particles within the atmospheric boundary layer, *Atmos. Meas. Tech.*, 8, 1627-1639, 2015.
- Bates, T. S., Quinn, P. K., Johnson, J. E., Corless, A., Brechtel, F. J., Stalin, S. E., Meinig, C., and Burkhardt, J. F.:
5 Measurements of atmospheric aerosol vertical distributions above Svalbard, Norway, using unmanned aerial systems (UAS), *Atmos. Meas. Tech.*, 6, 2115–2120, 2013.
- Boy, M., Hellmuth, O., Korhonen, H., Nilsson, E. D., ReVelle, D., Turnipseed, A., Arnold, F., and Kulmala, M.: MALTE – model to predict new aerosol formation in the lower troposphere, *Atmos. Chem. Phys.*, 6, 4499–4517, doi:10.5194/acp-6-4499-2006, 2006.
- 10 Cheung, H. C., Wang, T., and Baumann, K.: Influence of regional pollution outflow on the concentrations of fine particulate matter and visibility in the coastal area of southern China, *Atmos. Environ.*, 39, 6463-6474, 2005.
- Clarke, A. D., Ahlquist, N. C., Howell, S., and Moore, K.: A miniature optical particle counter for in situ aircraft aerosol research, *J. Atmos. Ocean. Tech.*, 19, 1557–1566, 2002.
- Davidson, C. I., Phalen, R. F., and Solomon, P. A.: Airborne particulate matter and human health: a review, *Aeros. Sci.*
15 *Tech.*, 39, 737-749, 2005.
- Day, D. E., W. C. Malm, and Kreidenweis, S. M.: Aerosol Light Scattering Measurements as a Function of Relative Humidity, *J. Air Waste Manage.*, 50, 710-716, 2000.
- Ding, A., Wang, T., and Xue, L.: Transport of north China air pollution by midlatitude cyclones: Case study of aircraft measurements in summer, *J. Geophys. Res.*, 114, 2009.
- 20 Ding, G. A., Chen, Z. Y., and Gao, Z. Q.: Vertical Distribution and Its Dynamic Characteristics of PM_{2.5} and PM₁₀ in Lower Atmosphere in Beijing, *Sci. China, Ser. D*, 35, 31-44, 2005.
- Dominici, F., Peng, R. D., Bell, M. L., Pham, L., McDermott, A., Zeger, S. L., and Samet, J. M.: Fine particulate air pollution and hospital admission for cardiovascular and respiratory diseases, *Jama*, 295, 1127-1134, 2006.
- Harnisch, F., Gohm, A., Fix, A., Schnitzhofer, R., Hansel, A., and Neisinger, B.: Spatial distribution of aerosols in the Inn
25 Valley atmosphere during wintertime, *Meteorol. Atmos. Phys.*, 103, 1–4, 223–235, 2009.
- Illingworth, S. M., Allen, G., Percival, C., Hollingsworth, P., Gallagher, M. W., Ricketts, R., Hayes, H., Ladosz, P., Crawley, D., and Roberts, G.: Measurement of boundary layer ozone concentrations on-board a Skywalker Unmanned Aerial Vehicle, *Atmos. Sci. Lett.*, 15, 4, 252–258, doi:10.1002/asl2.496, 2014.
- Liao, X., Zhang, X., and Wang, Y.: Comparative Analysis on Meteorological Condition for Persistent Haze Cases in
30 Summer and Winter in Beijing. *Environ. Sci.*, 35, 2031-2044, 2014.
- Maletto, A., McKendry, I. G., and Strawbridge, K. B.: Profiles of particulate matter size distributions using a balloon-borne lightweight aerosol spectrometer in the planetary boundary layer, *Atmos. Environ.*, 37, 661-670, 2003.



- Mamouri, R. E., Nisantzi, A., Hadjimitsis, D. G., Ansmann, A., Schwarz, A., Sasart, S., and Baldasano, J. M.: Complex vertical layering and mixing of aerosols over the eastern Mediterranean: active and passive remote sensing at the Cyprus University of Technology. In First International Conference on Remote Sensing and Geoinformation of Environment, Int. Soc. Opt. Photon, 879517-879517, 2013.
- 5 McKendry, I. G., Sturman, A. P., Vergeiner, J.: Vertical profiles of particulate matter size distributions during winter domestic burning in Christchurch, New Zealand, *Atmos. Environ.*, 38, 4805-4813, 2004.
- Ouyang, Y.: China wakes up to the crisis of air pollution, *Lancet Respir. Med.*, 1,12, 2013.
- Padró-Martínez, L. T., Patton, A. P., and Trull, J. B., Zamore, W., Brugge, D., Durant, J. L.: Mobile monitoring of particle number concentration and other traffic-related air pollutants in a near-highway neighborhood over the course of a year, 10 *Atmos. Environ.*, 61, 253-264, 2012.
- Peng, Z. R., Wang, D., Wang, Z., Gao, Y., Lu, S.: A study of vertical distribution patterns of PM_{2.5} concentrations based on ambient monitoring with unmanned aerial vehicles: a case in Hangzhou, China, *Atmos. Environ.*, 123, 357–369, doi:10.1016/j.atmosenv.2015.10.074, 2015.
- Pope, C. A., Burnett, R. T., Krewski, D., Jerrett, M., and Shi, Y.: Cardiovascular mortality and exposure to airborne fine 15 particulate matter and cigarette smoke shape of the exposure-response relationship, *Circ.*, 120, 941-948, 2009.
- Pope, C. A., Burnett, R. T., Thun, M. J., Calle, E. E., Krewski, D., Ito, K., and Thurston, G. D.: Lung cancer, cardiopulmonary mortality, and long-term exposure to fine particulate air pollution, *Jama*, 287, 1132-1141, 2002.
- Ramana, M., Ramanathan, V., Kim, D., Roberts, G. C. and Corrigan, C. E.: Albedo, atmospheric solar absorption and heating rate measurements with stacked UAVs, *Q. J. Meteor. Soc.*, 133, 1913-1931, 2007.
- 20 Ramanathan, V., M. V. Ramana, G. Roberts, D. Kim, C. Corrigan, C. Chung, and D. Winker. Warming trends in Asia amplified by brown cloud solar absorption, *Nature*, 448, 575-578, 2007.
- Šmíd, V., and Hofman, R.: Tracking of atmospheric release of pollution using unmanned aerial vehicles, *Atmos. Environ.*, 67, 425-436, 2013.
- Strawbridge, K. B., and Snyder, B. J.: Daytime and nighttime aircraft lidar measurements showing evidence of particulate 25 matter transport into the northeastern valleys of the Lower Fraser Valley, BC, *Atmos. Environ.*, 38, 5873-5886, 2004.
- Thomas, R. M., Lehmann, K., Nguyen, H., Jackson, D. L., Wolfe, D., and Ramanathan, V.: Measurement of turbulent water vapor fluxes using a lightweight unmanned aerial vehicle system, *Atmos. Meas. Tech.*, 5, 243–257, doi:10.5194/amt-5-243-2012, 2012.
- Van den Kroonenberg, A., Martin, T., Buschmann, M., Bange, J., and Vörsmann, P.: Measuring the wind vector using the 30 autonomous mini aerial vehicle M2AV, *J. Atmos. Ocean. Tech.*, 25, 1969–1982, 2008.
- Wang, W., Ma, J., and Hatakeyama, S.: Aircraft measurements of vertical ultrafine particles profiles over Northern China coastal areas during dust storms in 2006[J]. *Atmos. Environ.*, 425715-5720, 2008.



Wildmann, N., and Kaufmann, F., and Bange, J.: An inverse modelling approach for frequency response correction of capacitive humidity sensors in ABL research with small unmanned aircraft, *Atmos. Meas. Tech.*, 7, 4407–4438, doi:10.5194/amtd-7-4407-2014, 2014a.

5 Wildmann, N., Hofstätter, M., Weimer, F., Joos, A., and Bange, J.: MASC—a small remotely piloted aircraft (RPA) for wind energy research, *Adv. Sci. Res.*, 11, 55–61, doi:10.5194/asr-11-55-2014, 2014b.

Wildmann, N., Mauz, M., and Bange, J.: Two fast temperature sensors for probing of the atmospheric boundary layer using small remotely piloted aircraft (RPA), *Atmos. Meas. Tech.*, 6, 8, 2101–2113, doi:10.5194/amt-6-2101-2013, 2013.